NeuroImage 125 (2016) 522–532

Contents lists available at ScienceDirect

NeuroImage

journal homepage: www.elsevier.com/locate/ynimg

Brain–robot interface driven plasticity: Distributed modulation of corticospinal excitability

Dominic Kraus [a,b], Georgios Naros [a,b], Robert Bauer [a,b], Maria Teresa Leão [a,b], Ulf Ziemann [c], Alireza Gharabaghi [a,b,*]

[a] Division of Functional and Restorative Neurosurgery & Division of Translational Neurosurgery, Department of Neurosurgery, Eberhard Karls University Tuebingen, Germany
[b] Neuroprosthetics Research Group, Werner Reichardt Centre for Integrative Neuroscience, Eberhard Karls University Tuebingen, Germany
[c] Department of Neurology and Stroke, and Hertie Institute for Clinical Brain Research, Eberhard Karls University Tuebingen, Germany

ARTICLE INFO

Article history:
Received 14 July 2015
Accepted 24 September 2015
Available online 24 October 2015

Keywords:
Brain–computer interface
Brain–machine interface
Brain–robot interface
EEG
Event-related desynchronization
Plastic reorganization
Stimulus–response curve
Corticospinal excitability

ABSTRACT

Brain–robot interfaces (BRI) are studied as novel interventions to facilitate functional restoration in patients with severe and persistent motor deficits following stroke. They bridge the impaired connection in the sensorimotor loop by providing brain-state dependent proprioceptive feedback with orthotic devices attached to the hand or arm of the patients. The underlying neurophysiology of this BRI neuromodulation is still largely unknown.

We investigated changes of corticospinal excitability with transcranial magnetic stimulation in thirteen right-handed healthy subjects who performed 40 min of kinesthetic motor imagery receiving proprioceptive feedback with a robotic orthosis attached to the left hand contingent to event-related desynchronization of the right sensorimotor cortex in the β-band (16–22 Hz). Neural correlates of this BRI intervention were probed by acquiring the stimulus–response curve (SRC) of both motor evoked potential (MEP) peak-to-peak amplitudes and areas under the curve. In addition, a motor mapping was obtained. The specificity of the effects was studied by comparing two neighboring hand muscles, one BRI-trained and one control muscle.

Robust changes of MEP amplitude but not MEP area occurred following the BRI intervention, but only in the BRI-trained muscle. The steep part of the SRC showed an MEP increase, while the plateau of the SRC showed an MEP decrease. MEP mapping revealed a distributed pattern with a decrease of excitability in the hand area of the primary motor cortex, which controlled the BRI, but an increase of excitability in the surrounding somatosensory and premotor cortex.

In conclusion, the BRI intervention induced a complex pattern of modulated corticospinal excitability, which may boost subsequent motor learning during physiotherapy.

Introduction

Restitution of useful function in patients with severe and persistent motor deficits following stroke is very limited. Conventional therapies are based on physiotherapy, which mostly relies on some degree of residual movement and is therefore often restricted in patients with severe motor impairment. For such patients novel therapeutic strategies, including robot-assisted training, are investigated to facilitate rehabilitation (Langhorne et al., 2009; Mehrholz et al., 2012).

More recent approaches include direct patient control, i.e. brain interfacing, over the robotic training devices by motor imagery-related sensorimotor oscillations of the ipsilesional cortical electroencephalogram (Ang et al., 2011, 2015; Buch et al., 2008, 2012; Gomez-Rodriguez et al., 2011; Pichiorri et al., 2015; Prasad et al., 2010; Ramos-Murguialday et al., 2013; Shindo et al., 2011). While *assistive* brain–machine interfaces (BMI) aim to replace lost function by controlling external devices, the goal of *restorative* BMI is to rehabilitate the respective function (Bauer and Gharabaghi, 2015a,b; Naros and Gharabaghi, 2015). In such a restorative framework, BMI provide contingent feedback to facilitate self-regulation of brain activity that is considered beneficial for recovery. When used in conjunction with robotic rehabilitation technology, these devices are also referred to as brain–robot interfaces (BRI; Bauer et al., 2015; Vukelić and Gharabaghi, 2015a,b).

These brain–robot interfaces (BRI) bridge the impaired connection in the sensorimotor loop by providing brain-state dependent proprioceptive feedback with orthotic devices attached to the hand or arm of the patients. Such supported movements facilitate the detection of motor intention even in the absence of actual movements (Gomez-Rodriguez et al., 2011) and have revealed promising pilot results in stroke survivors (Ang et al., 2011, 2015; Prasad et al., 2010; Ramos-Murguialday et al., 2013; Shindo et al., 2011).

Within a complex network of factors, incorporating the affected hand in activities of daily living by volitional finger extension is an important

* Corresponding author at: Division of Functional and Restorative Neurosurgery & Division of Translational Neurosurgery, Department of Neurosurgery, Eberhard Karls University, Otfried-Mueller-Str.45, 72076 Tuebingen, Germany. Fax: +49 7071 29 25104.
E-mail address: alireza.gharabaghi@uni-tuebingen.de (A. Gharabaghi).

http://dx.doi.org/10.1016/j.neuroimage.2015.09.074
1053-8119/

determinant of quality of life for severely affected patients and is therefore predominantly targeted by therapeutic interventions (Dobkin, 2005; Clarke and Black, 2005; Kutner et al., 2010). Relevant functional improvement of the hand and finger function is however still missing in the patient group with persistent deficits of the upper limb even when applying novel techniques such as BRI training combined with physiotherapy. This has drawn interest in the specificity and mechanisms of BRI therapy, particularly because the underlying neurophysiology of training with a BRI hand orthosis is still largely unknown.

The current concept assumes associative learning by the connection between the neural correlates of movement intention and the contingent feedback, thereby inducing a priming effect of BRI training for immediately following physiotherapy (Ramos-Murguialday et al., 2013; Pichiorri et al., 2015). Such a mechanism of boosting subsequent use-dependent plasticity would however necessitate – according to the principles of homeostatic metaplasticity – a *decrease* of neuronal activity in the motor cortex before the physiotherapy practice (Ziemann and Siebner, 2008). In contrast, brain–interface based neurofeedback interventions have shown an *increase* of corticospinal excitability evaluated by transcranial magnetic stimulation (TMS) and motor evoked potentials (MEP) (Mokienko et al., 2013; Pichiorri et al., 2011; Shindo et al., 2011). These measurements, however, did not provide a complete sensorimotor map including a full stimulus–response curve (Mokienko et al., 2013; Pichiorri et al., 2011; Shindo et al., 2011). Moreover, recent methodological improvements of TMS mapping allow meanwhile accounting for the individual gyral anatomy and decreasing the variability of cortical motor maps (Kraus and Gharabaghi, 2015). Such a refined and extended mapping, however, might be particularly relevant since recent studies revealed that BRI interventions may entrain an extended cortical motor network (Vukelić and Gharabaghi, 2015a) with distributed, but spatially selective and frequency specific effects on cortico-cortical connectivity lasting beyond the intervention period (Vukelic and Gharabaghi, 2015b).

We hypothesized that these cortical modulations would result in distributed, but specific and robust changes of corticospinal connectivity as well, with the largest MEP gains in those areas modulated strongest by the feedback intervention.

In the present study, we therefore performed a detailed analysis of the functional topography of corticospinal connectivity, i.e. mapping the whole sensorimotor cortex including primary motor, somatosensory and higher motor areas, while comparing two neighboring forearm muscles, i.e. one BRI trained and one control muscle. Finally, we sought to unravel the neural mechanisms by analyzing both the peak-to-peak amplitudes and the respective area under the MEP curve, i.e. disentangling whether the observed changes were mediated by higher synchronicity of the engaged neuronal population or by the recruitment of additional neuronal pools.

Materials and methods

Subjects

Thirteen healthy subjects (mean age, 24.2 ± 2.5 years, range 19–28 years, nine male) with no history of neurological or psychiatric disease and no contraindications to TMS (Rossi et al., 2009) participated in this study. All were right-handers confirmed with the Edinburgh Handedness Inventory (Oldfield, 1971). The study was approved by the local ethics committee and all subjects gave written informed consent prior to participation. Participants were seated in a comfortable reclining chair for the duration of the whole experiment.

Recordings

EMG

Electromyographic (EMG) activity was recorded from left the Extensor Digitorum Communis (EDC) and the left Extensor Carpi Radialis (ECR) muscle using Ag/AgCl AmbuNeuroline 720 wet gel surface electrodes (Ambu GmbH, Germany) placed 2 cm apart on either muscle belly. We localized each of the two muscles based on anatomical landmarks and muscle palpation during passive and active wrist and finger extension, respectively. After filtering between 0.16 Hz and 1 kHz, EMG was recorded with 5 kHz sampling rate and downsampled to 1 kHz by the BrainAmp ExG Amplifier (Brainproducts GmbH, Germany) before transmission of the signals to the BCI2000 software (Schalk et al., 2004). For the TMS mapping (see below) before and after the experiment the integrated 6 channel EMG device of the eXimia Navigated Brain Stimulation (NBS) system (Nexstim Inc., Finland) was used with a 3 kHz sampling rate and a band-pass filter of 10–500 Hz.

EEG

Electroencephalographic (EEG) signals were recorded during the whole experiment in a 32 channel setup according to the international 10–20 system (Fp1, Fp2, F3, Fz, F4, FT7, FC5, FC3, FC1, FC2, FC4, FC6, FT8, C5, C3, C1, Cz, C2, C4, C6, TP7, CP5, CP3, CP1, CPz, CP2, CP4, CP6, TP8, P3, P4, POz, with FCz as reference) using Ag/AgCl electrodes and BrainVision software with DC Amplifiers (BrainAmp, Brainproducts GmbH, Germany). All impedances were kept below 10 kΩ throughout the experiment. After filtering between 0.16 Hz and 1 kHz, EEG was recorded with 5 kHz sampling rate and downsampled to 1 kHz by the BrainAmp DC Amplifier (Brainproducts GmbH, Germany) before transmission of the signals to the BCI2000 software (Schalk et al., 2004) for online analysis and offline storage.

TMS mapping protocol

Anatomical T1 weighted magnetic resonance imaging (MRI) sequences were acquired for every subject before the first experiment using a 3-Tesla Siemens TIM Trio MRI system (Siemens AG, Germany) and were imported into the eXimia NBS system (eXimia®, Nexstim, Helsinki, Finland). For each subject the cortical representation of the EDC muscle of the left arm was determined using 40% of stimulator output of the navigated Nexstim eXimia TMS stimulator with a biphasic single pulse coil (Focal Bipulse Coil (5 cm mean winding diameter)) and the anatomical defined 'hand knob' of the primary motor cortex (M1) as starting position. TMS over M1 evokes multiple descending volleys generated by direct (D wave) and indirect (I waves), i.e. via presynaptic neurons, activation of pyramidal tract neurons. MEPs at higher amplitudes are expected to reflect the recruitment of these additional presynaptic neuronal pools, e.g. later I waves. Moreover, biphasic pulses are expected to activate this larger set of neurons in comparison to monophasic stimulation (Di Lazzaro et al., 2001) allowing probing their modulation by the intervention. At the same time biphasic instead of monophasic stimulation allows to evoke MEPs with less energy injection thereby improving the focality and sensitivity (Raffin et al., 2015). If the starting stimulator output was not sufficient to elicit motor evoked potentials (MEPs), the stimulator output was increased in 5% steps. The current waveform of the stimulator was biphasic with the orientation of the induced current in the brain posterior–anterior for the first phase and anterior–posterior for the second phase of the stimulus. The orientation of the electric field, calculated with the individual MRI of each subject by the NBS software, was kept perpendicular to the central sulcus as a starting position and the location with the highest MEP response was selected as the stimulation point. After determining the 'hotspot' by moving the coil around the hand knob, the orientation of the coil was refined and varied in roughly 10° steps around the original orientation to determine the orientation with the highest response in this spot. Resting motor threshold (RMT) was determined using the relative frequency method, i.e. selecting the minimum stimulus intensity (closest 2% of maximum stimulator output (MSO)) that resulted in MEPs > 50 μV in the peak-to-peak amplitude in at least 5 out of 10 consecutive trials (Groppa et al., 2012; Ziemann et al., 1996). To test for changes in corticospinal excitability, we acquired a MEP stimulus–

response curve at the 'hotspot'. The intensities for the MEP stimulus–response curve were calculated with the estimated electrical field of the NBS system at the 'hotspot' in a depth of ~22 mm (Danner et al., 2008; 2012). For each subject the starting intensity was at 60% RMT and increased in steps of 10 V/m. For each intensity step, 10 MEPs were recorded. Additionally, a cortical map representation was acquired at 110% RMT. This map was extended around the hot spot with evenly distributed stimuli till no MEPs could be evoked in the EDC or ECR. A visual grid ($5 \times 5 \times 5$ mm) predefined in the navigation software was used for guidance during the mapping procedure. The order of grid cells selected for stimulation was randomized across subjects. Both the inter-stimulus interval and the inter-site interval had a natural jitter of up to seconds as every stimulation pulse was initiated by the examiner via a food pedal while visually monitoring both the evoked response as well as the coil position, orientation and tilting with the help of the navigation system.

For data analyses we then used the actual navigation coordinates of each stimulus resulting in a spacing of approximately 3 mm. For visualization, these spots were finally interpolated and sampled on a $1 \times 1 \times 1$ mm grid to close the gap between stimulation sites and then projected onto the gyral anatomy to decrease the variability of the cortical motor maps following a procedure described recently in detail elsewhere (Kraus and Gharabaghi, 2015). This led to ~100 stimuli applied during the mapping. For all TMS measurements, subjects were instructed to keep muscles relaxed. The procedure lasted for ~15 min (see Fig. 1a). During offline analysis, the EMG data were visually inspected and trials were discarded from analysis, when muscle preactivation was present (<1% of all trials had to be removed due to EMG activation).

Abolition of transient effects by a depotentiation task

As already 150 stimuli have been shown to induce transient plastic changes of corticospinal excitability (Touge et al., 2001), we included a finger flexion and extension task following the first TMS mapping to abolish these effects (Todd et al., 2009). This depotentiation task consisted of 30 repetitions of flexion/extension. After a 5 min rest period the BRI intervention followed and lasted for approximately 40 min. Any influence of the depotentiation task on the BRI intervention following the principles of homeostatic metaplasticity is therefore unlikely, particularly since the task itself has been shown to modify subsequent motor evoked potentials only when proceeded by neuromodulation (Goldsworthy et al., 2015).

This very same depotentiation task was repeated immediately after the intervention to eliminate transient effects as well and to probe for the robustness of induced corticospinal excitability (Goldsworthy et al., 2015). During this depotentiation task a bar on a computer screen was rhythmically drifting up and down. Subjects had to match this bar with a ball on the screen that was controlled by finger flexion and extension mediated via an attached hand orthosis (Amadeo®, Tyromotion GmbH, Austria). An extension of the fingers resulted in an upward movement, whereas a flexion resulted in a downward movement. Whenever the ball was matching the moving bar, it turned from red to green. Therefore, following this depotentiation task, any changes measured with the TMS mapping after the intervention (BRI training, see below) can be considered as robust changes of corticospinal excitability resistant to depotentiation (Goldsworthy et al., 2015).

Experimental condition

The general design of the experiment is illustrated in Fig. 1a. The experiment started with the TMS mapping, followed by the depotentiation task (5 min) and a rest period (5 min). These different epochs were separated by approximately 2 min to change between setups. The intervention consisted of 15 runs. Each run lasted approximately 2.5 min and included 11 trials. Each trial started with a 2 s preparation phase, followed by a 6 s motor imagery phase, and a 6 s rest phase. During the motor imagery phase subjects were instructed to perform kinesthetic motor imagery, i.e. to imagine the feeling of opening their left hand from a first person perspective, and to keep muscles relaxed during this intervention. More specifically, subjects were asked to perform motor imagery of finger extension (and not wrist extension), a task that is specifically addressing the EDC (and not the ECR). Moreover, the hand robot was selectively extending the fingers, while the wrist remained fixed by a Velcro strap without any movement. Online EMG monitoring of both muscles throughout the whole experiments confirmed the immobilization of the ECR. Pilot stroke rehabilitation data indicates that the very same intervention, as applied in this study, may indeed result in muscle specific improvements of the finger as compared to the wrist function (Naros and Gharabaghi, 2015).

During the experiments, the EMG was visually inspected by experienced examiners who excluded trials with movements. Additionally, repetitive activities larger than 50 μV during the motor imagery phase were discarded offline. This was necessary in less than 1% of all trials. To further exclude the influence of small muscle activations, an offline correlation analysis between EMG activity during the motor imagery task and the pre/post intervention MEP changes was performed and found no interaction.

Preparation and imagery phases were initiated by the audiotaped cues of a female voice 'left hand' and 'go', respectively. After the intervention and another depotentiation task (5 min), a second TMS mapping followed (Fig. 1a).

Passive opening of the left hand was delivered by a robotic hand orthosis (Amadeo®, Tyromotion GmbH, Austria) and was initiated by the BCI2000 software after detection of event related desynchronization (ERD) in the β-band (16–22 Hz) during motor imagery (Gharabaghi et al., 2014). ERD was analyzed at electrodes FC4, C4 and CP4 over the right sensorimotor area during the motor imagery phase (McFarland et al., 2000). A full opening of the hand orthosis was achieved when ERD was maintained for 5 s. Movement stopped as soon as ERD was absent (Fig. 1b). The frequency power was estimated by an autoregressive model with a model order of 16 based on the Burg Algorithm (McFarland and Wolpaw, 2008). A linear classifier with nine features consisting of three channels (FC4, C4, and CP4) and three independent 2-Hz frequency bins for estimation of spectral power from 16 to 22 Hz were used to detect decreases in sensorimotor rhythm power in the β-band. To ensure robotic movements only during sufficiently long periods of ERD, five consecutive 40 ms epochs had to be classified as ERD to initiate hand opening by the orthosis. Three calibration runs were performed before the experiment to implement an individual desynchronization threshold and to consider each subject's ability for desynchronization. This assured that each subject was facing the same task-related demand. During the intervention feedback was given only when subjects reached 20% of their strongest beta-ERD modulation in the motor-imagery epoch (Gharabaghi et al., 2014). Whenever

Fig. 1. a) Schematic illustration of the experimental design and timeline (for details, please see Materials and Methods). b) Exemplary raw data of EMG recordings of the EDC (μV, left y-axis, red) and the online EEG classifier output (ß-power from 16 to 22 Hz in arbitrary units, right y-axis, black) for a single trial. Please note: When a predefined threshold of ß-ERD is reached (gray horizontal line) during the motor imagery phase (i.e. after the "go" signal, 0–6 s) the subject's hand is passively opened via the robotic orthosis (indicated as a blue line at the top). This robot assisted movement stops as soon as the ß-ERD is not sufficient to reach the threshold. After the "relax" command the orthosis closes the hand again (indicated as a red line at the top). c) Focal topography of event-related spectral perturbation during the motor imagery phase, averaged across all trials of all subjects, with blue colors indicating desynchronisation relative to rest with units in standard deviations.

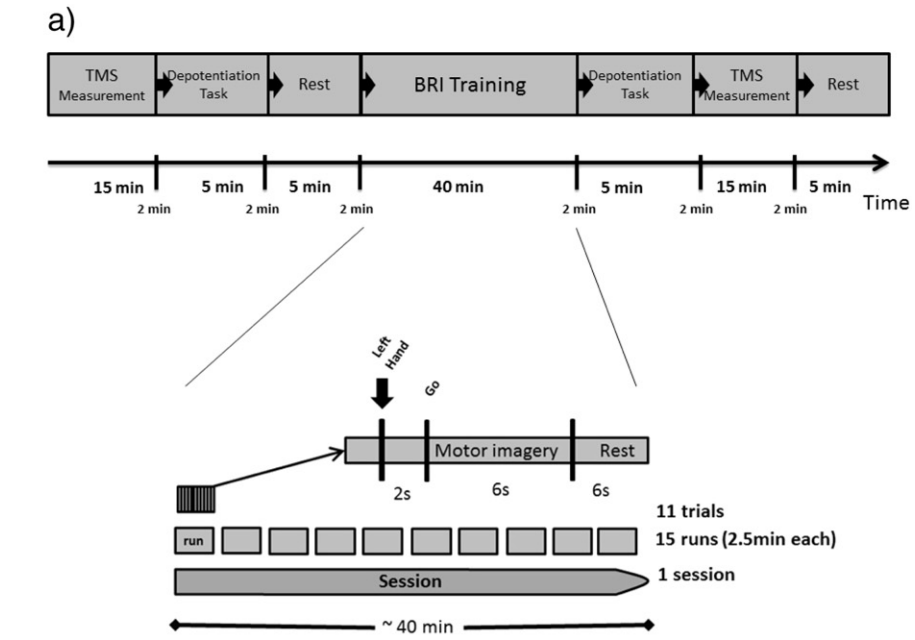
a)
TMS Measurement
Depotentiation Task
Rest
BRI Training
Depotentiation Task
TMS Measurement
Rest
15 min
2 min
5 min
2 min
5 min
2 min
40 min
2 min
5 min
2 min
15 min
2 min
5 min
Time
Left Hand
Go
Motor imagery
Rest
2s
6s
6s
11 trials
run
15 runs (2.5min each)
Session
1 session
~ 40 min

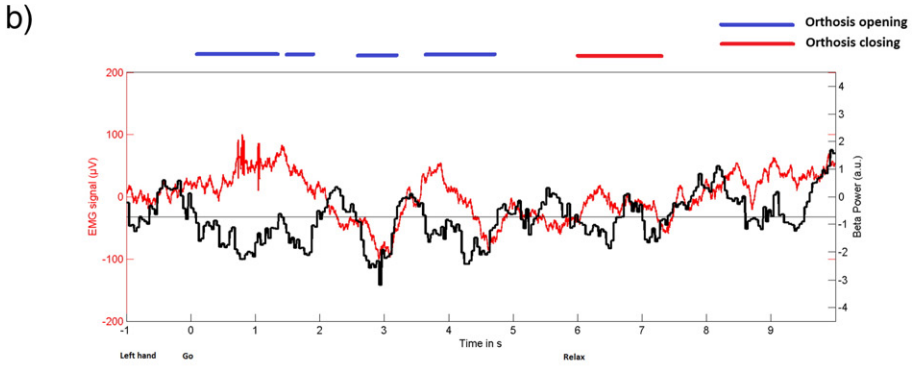
b)
Orthosis opening
Orthosis closing
EMG signal (uV)
Beta Power (a.u.)
Time in s
Left hand
Go
Relax

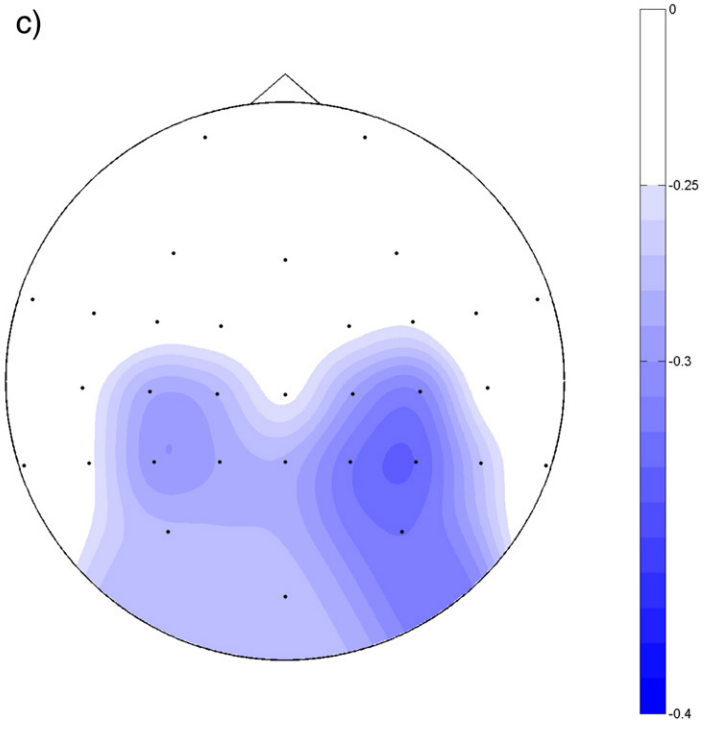
c)
0
-0.25
-0.3
-0.4

the threshold was not met due to insufficient event-related desynchronization either no robotic opening of the hand occurred or ongoing robotic opening stopped, but could be reinitiated in the same trial if the threshold was met again. The orthosis moved back to the 'hand closed' position after the 'relax' command within the first 1.5 s of the rest phase (Fig. 1b).

Data analysis

Data were analyzed using Matlab R2010b (Mathworks) with a custom built code and SPSS V21 (IBM).

Stimulus–response curve (SRC)

A repeated measure ANOVA (rmANOVA) with time (pre- and post-intervention), intensity (4 levels, see below) and muscle (EDC, ECR) as within-subject effect, was performed for MEP peak-to-peak amplitude and MEP area of the binned data (bins: 71–90% RMT, 91–110% RMT, 111–130% RMT, 131–160% RMT) of the individual mean MEP amplitudes. In the case of a violation of sphericity a Greenhouse–Geisser correction was performed. Post-hoc testing was done as described below for the different parameters of the SRC.

A three parameter Boltzmann sigmoidal function was fitted using Eq. (1) (Devanne et al., 1997; Houdayer et al., 2008; Möller et al., 2009) for the peak-to-peak MEP amplitude curve and Eq. (2) was applied for the area under the MEP curve, separately for the pre and post responses of all subjects. A robust fit was performed using a Huber weighted least square method to compensate for heteroscedasticity and outliers, which means that in each fitting iteration step the weight of a response was decreased linearly with its distance from the curve (Huber, 1981).

$$MEP(S) = MEPmax/(1 + \exp(k(S50 - S))) \quad (1)$$

$$MEParea(S) = MEPmaxarea/(1 + \exp(m(Sarea50 - S))). \quad (2)$$

In Eqs. (1) and (2), MEP(S) represents the mean peak-to-peak MEP, and MEParea(S) represents the mean area under the MEP curve elicited by a stimulus intensity S. MEPmax and MEPmax area represent the saturation amplitude of the peak-to-peak MEP amplitude and the MEP area, respectively. S50 and Sarea50 stand for the stimulation intensity needed to obtain 50% of MEPmax and MEPmax/area, respectively. k and m are the slope parameters which represent the recruitment gain in the corticospinal pathway. The inverse of the slope parameters (1/k; 1/m) is directly proportional to the maximal steepness of the function, which occurs at S50/Sarea50, i.e. the steepness reflects the slope at the point of inflexion (Devanne et al., 1997).

This procedure resulted in a mean SRC of all subjects pre- and post-intervention. A 95% confidence interval was calculated for each curve parameter and for the curves. The 95% confidence intervals of the pre- and post-intervention SRCs were then compared to each other by calculating the difference of their means and the corresponding 95% confidence intervals. Both pre- and post-intervention curve parameters and the differences between interventions (percentage changes) were then tested for significance using the method described by Altman and Bland (2011). P values for the differences in MEPmax, MEPmax/area, S50, Sarea50, m and k were calculated and Bonferroni corrected for multiple comparison ($\alpha = 0.008$).

RMT and map parameters

All stimulation points of the cortical map were projected from the scalp onto the cortex. This projection was performed along the coil axis in the direction of the magnetic field using the coil coordinates acquired by the navigation system. Subsequently the MEPs of all applied stimuli were 3D-interpolated on a 1 × 1 × 1 mm grid. The resulting map area (with responses above 50 μV) was obtained for each pre- and post-intervention measurement. Thereafter, we calculated the following parameters: Mean MEP of the map, number of active grid cells (Area) and center of gravity (CoG) displacements in latitude and longitude directions (Wassermann et al., 1992). Additionally, a repeated measures ANOVA was performed for changes in map parameters (mean MEP, area and CoG) and RMT for within subject effects of time (pre, post) and muscle (EDC, ECR).

Correlation of SRC change with ERD performance

A partial correlation analysis was performed for the post-versus pre intervention changes of the SRC with the EMG background activity, ERD duration and changes in ERD power during the intervention. The ERD power (15–30 Hz) was calculated for the electrodes C2/C4 and CP2/CP4, respectively, comparing the first two with the last two runs of the session.

Topographic spectral power analysis

Spectral power (Fig. 1c) was calculated offline for the period of 3 s before to 8 s after the start of motor imagery phase. Every trial was band-pass filtered between 14 and 26 Hz followed by wavelet convolution for the frequency range from 16 to 22 Hz in steps of 100 ms. Based on the mean and standard deviation of the band power during the baseline period (i.e. seconds −3 to 0), we calculated the relative power modulation and averaged this event-related spectral perturbation for the motor imagery phase (i.e. seconds 0 to 6).

Results

We found muscle specific and robust changes of motor evoked potentials (MEP) following the intervention. The steep part (around the MEP threshold and the inflexion of the SRC) and the plateau (maximum MEP) of the SRC revealed opposite effects with increases and decreases of corticospinal excitability, respectively. More specifically, rmANOVA after Greenhouse–Geisser correction of the peak-to-peak stimulus response curve revealed a significant effect of muscle ($F1, 12 = 11.31$; $p = 0.006$), intensity ($F1.59, 19.05 = 56.76$; $p < 0.001$), time ($F1, 12 = 5.36$; $p = 0.039$), an interaction of muscle × intensity ($F1.6, 19.2 = 3.96$; $p = 0.044$) and an interaction of muscle × intensity × time ($F2.01, 24.15 = 3.59$; $p = 0.043$). For the MEP area SRC, rmANOVA after Greenhouse–Geisser correction showed only a significant effect of muscle ($F1, 12 = 5.445$; $p = 0.038$) and intensity ($F1.66, 19.96 = 18.67$; $p < 0.001$), but not for time or any interaction. A post-hoc test of the peak-to-peak stimulus response parameters showed a significant change in MEPmax, S50 and k in the EDC muscle (Fig. 2a), but no significant difference for the ECR muscle (Fig. 2b) revealing specificity of the intervention. The MEP area stimulus response parameters did not show any changes for either muscle (Figs. 2c, d). The MEP increase in the steep part of the SRC correlated with frequency-specific and more pronounced mean β-ERD of individual participants for CP2/CP4 ($rho = -0.74$; $p = 0.023$) (Fig. 3) but not for C2/C4. There was no correlation with the ERD duration (average of 17.3 s ± 4.1 s per run during the motor imagery phase) or the EMG background activity (mean of 40.7 μV ± 2.8 μV).

Changes in Boltzmann parameters are summarized in Fig. 4a for the EDC muscle and in Fig. 4b for the ECR muscle. MEPmax of the EDC muscle decreased to 65% of pre-intervention baseline ($p < 0.0001$), S50 decreased to 85.7% of the baseline value ($p < 0.0001$) and slope k increased to 146.1% of pre-intervention baseline ($p < 0.0001$).

The topographic TMS maps revealed a distributed pattern of cortical plasticity with decreases of excitability in the M1 hand area that controlled the BRI, and increases of excitability in the surrounding cortical areas including the somatosensory and premotor cortex (Fig. 5).

The rmANOVA of the RMT and map parameters revealed a significant effect of time on the CoG location (MRI coordinates from the navigation system with the reference at the lower right corner of each individual MRI) in anterior–posterior direction ($F1, 12 = 8.58$; $p = 0.013$) (Table 1).

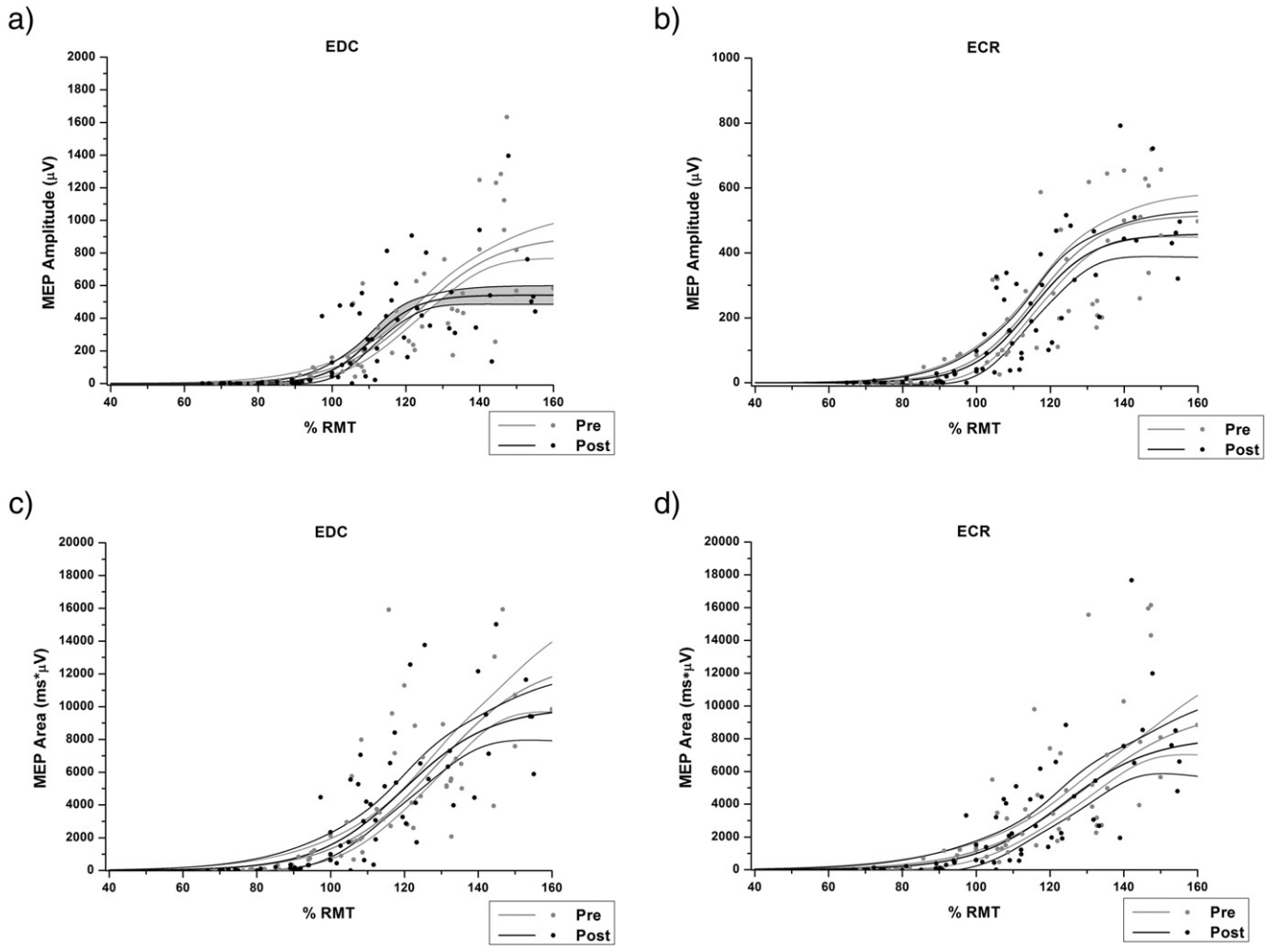

Fig. 2. Boltzmann fit of the mean MEP peak-to peak stimulus–response curves (in μV) pre intervention (light gray) and post intervention (black) for the EDC muscle (a) and the ECR muscle (b). Boltzmann fit of the mean MEP area stimulus–response curves (in μV ∗ ms) pre intervention (light gray) and post intervention (black) for the EDC muscle (c) and the ECR muscle (d). Thin lines indicate the 95% confidence intervals of the curves, shaded area represents the significant difference pre- versus post-intervention. Data points represent the raw MEP data points off all subjects.

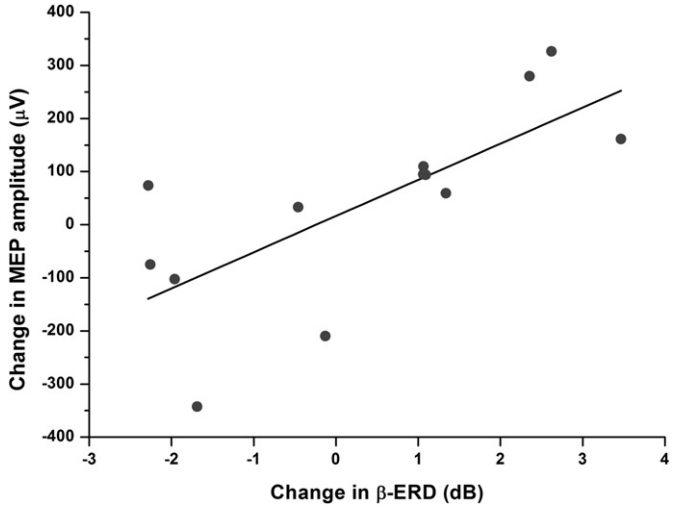

Fig. 3. Post-versus pre-intervention MEP changes for the EDC in the steep part of the SRC compared to changes in beta-ERD level of individual participants between the first two and the last two runs of the session recorded with CP2/CP4. More pronounced ERD (i.e. positive sign × values) led to stronger MEP increase.

Discussion

This study investigated changes of corticospinal excitability in healthy subjects who performed 40 min of kinesthetic motor imagery receiving proprioceptive feedback with a robotic hand orthosis contingent to event-related β-band desynchronization. One single brain–robot interface (BRI) session was already sufficient to induce a complex and robust pattern of modulated corticospinal excitability with opposing effects within both the stimulus–response curve and the sensorimotor cortex.

While classical *assistive* brain–computer interface (BCI)/ brain–machine interface (BMI) approaches choose a subject-specific frequency band and/or alpha frequency to maximize the classification accuracy e.g. between motor-imagery and rest, *rehabilitative* BRI/BMI approaches, such as the one used in this study, intend to restore the communication between cortex and periphery by operant conditioning of a specific brain-state. As this interaction is naturally mediated in the β-band, we selected this frequency band, which mediates the disinhibition of the sensorimotor cortex and the coherent interaction with the muscles (Kilavik et al., 2013; Kristeva et al., 2007; Mima et al., 2000; van Wijk et al., 2012), rather than the α-band which gates information by inhibiting task-irrelevant regions (Jensen and Mazaheri, 2010). Along these lines, self-regulation of the β-band has recently been

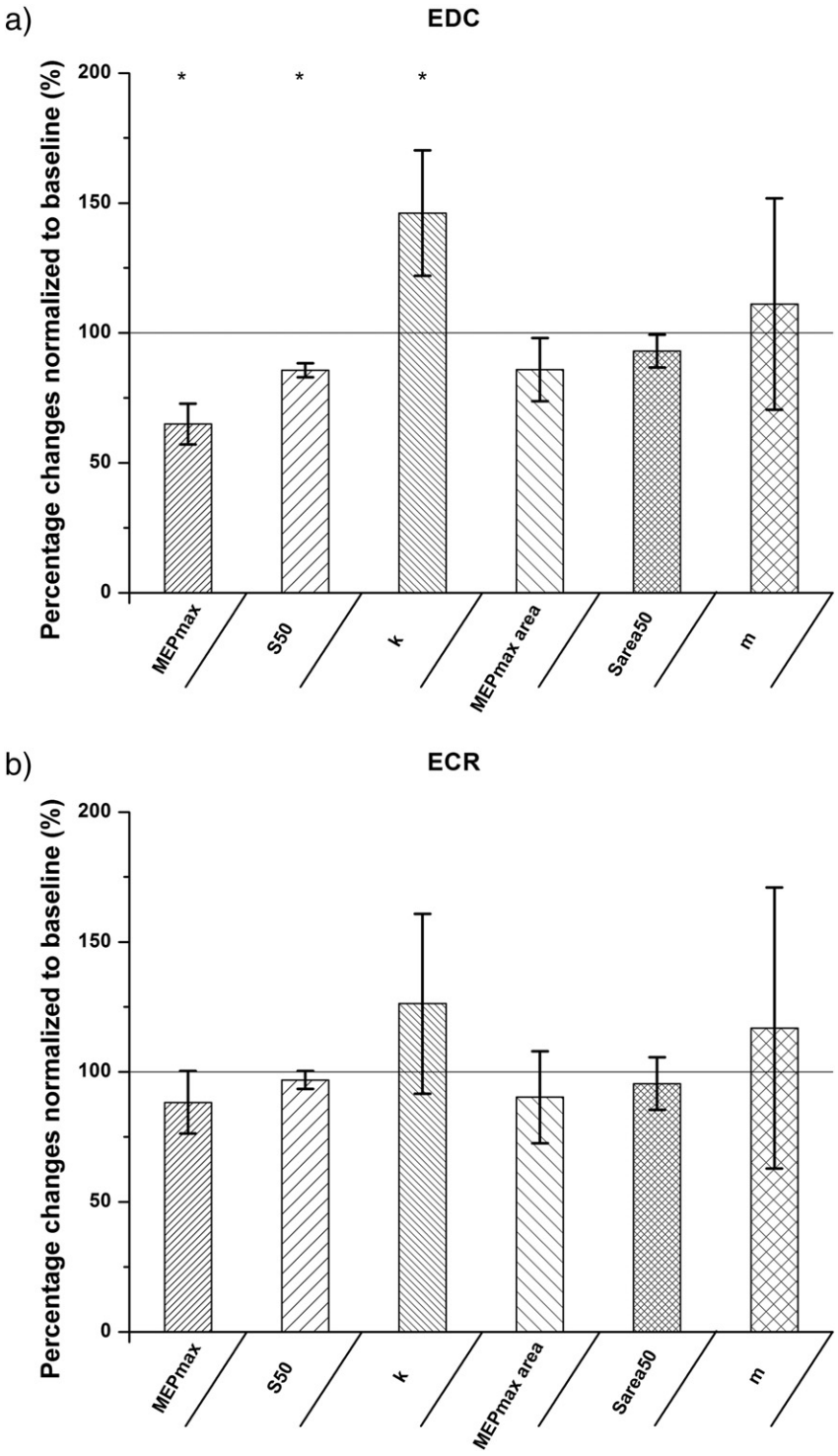

Fig. 4. Means of MEPmax, MEPmax area, S50, Sarea50, slope k and m post-intervention normalized to baseline (in %) for the EDC muscle (a) and the ECR muscle (b). Error bars indicate 95% confidence intervals. * significant differences pre- vs. post-intervention ($p < 0.008$).

shown to be facilitated by proprioceptive BRI feedback as compared to visual BCI feedback (Vukelić and Gharabaghi, 2015a), to activate the distributed cortical motor network (Vukelić et al., 2014) and to bridge the gap between the abilities and cortical networks of motor imagery and motor execution (Bauer et al., 2015). This intervention may even result in interhemispheric connectivity changes lasting beyond the intervention and modifying subsequent cortical resting networks (Vukelic and Gharabaghi, 2015b). Moreover, recent prove-of-concept data suggest that frequency-specific operant conditioning of β-band oscillations with BRI neurofeedback may lead to task-specific motor improvement in chronic stroke (Naros and Gharabaghi, 2015). The present study extended this line of research by probing the impact of this intervention on the effective connectivity to the periphery.

On the one hand, we replicated earlier findings indicating that brain-interface based neuromodulation *increases* corticospinal excitability for the steep part of the stimulus–response curve (SRC) at the hot-spot of the trained hand muscle (Mokienko et al., 2013; Pichiorri et al., 2011). The observations are in line with previous studies examining motor

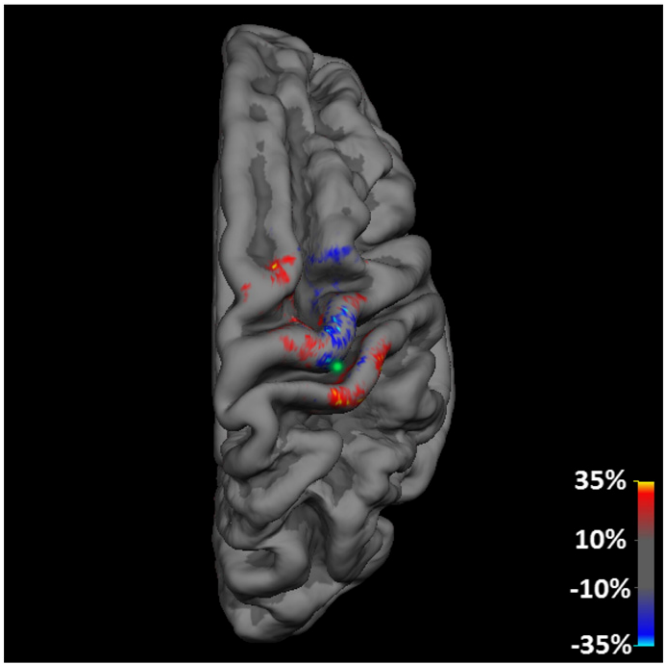

Fig. 5. Changes in cortical group TMS maps of the EDC post- versus pre-intervention. Color bar indicates percentage increases in MEP size (red/yellow) and decreases in MEP size (blue/turquoise). The green dot represents the 'hot spot', where the MEP stimulus response curve was acquired.

imagery and peripheral stimulation. Motor imagery has been shown to increase corticospinal excitability (Ridding and Rothwell, 1999; Roosink and Zijdewind, 2010; Stinear and Byblow, 2004; Stinear et al., 2006) and to decrease intracortical inhibition (Abbruzzese et al., 1999), phenomena which are both amplified when combined with afferent input (Ridding and Rothwell, 1999; Saito et al., 2013). Therefore, the current study focused on this combined intervention. On the other hand, we detected a significant *decrease* of corticospinal excitability at the same stimulation spot at higher stimulation intensities, i.e. at the plateau of the SRC, a finding not reported previously.

These changes in corticospinal excitability were muscle-specific, i.e. limited to the EDC muscle, which was involved in the motor imagery-related, orthotic hand opening, and were not present in the neighboring ECR muscle, which was not involved in the task and remained fixed throughout the experiment. This result is in line with muscle-specific changes in corticospinal excitability during both motor imagery (Rossini et al., 1999; Stinear and Byblow, 2004) and somatosensory input which was applied via electrical stimulation, passive movement or vibration (Kaelin-Lang et al., 2002; Macé et al., 2008; Rosenkranz et al., 2003; Rosenkranz and Rothwell, 2003, 2012). However, it should be noted, that the hotspot selection in the present study was performed for the EDC, and not the ECR, and has therefore influenced the respective SRC, i.e. resulting in lower maximum MEP for the latter. This can be explained by the larger distance of the induced electrical field from the cortical neurons responsible for ECR activation. *Relative* pre-post changes would have been captured by this ECR SRC as well despite the larger distance, i.e. lower *absolute* value of the mapping parameter. However, this *remote* ECR SRC might have been potentially less sensitive to changes. Future studies should therefore consider acquiring each SRC at the respective hotspots. Nonetheless, a selective modulation of EDC related spinal and/or cortical neuronal pools may well be explained by the proprioceptive input during robot mediated finger extension, i.e. addressing the EDC, while the wrist (ECR) remained fixed without any movement, and/or by motor imagery of finger extension and not wrist extension.

Table 1
Summary of RMT and map parameters before and after the intervention.

Measure	RMT (% MSO)	Mean MEP (μV)	Map area (cm^3)	CoG anterior–posterior (mm)	CoG lateral–medial (mm)
Pre					
ECR	43.9 ± 8.3	172.8 ± 106.3	1.71 ± 0.85	0	0
EDC	43.6 ± 8.6	235.2 ± 148.1	1.96 ± 0.99	0	0
Post					
ECR	44.8 ± 10.8	194.4 ± 134.7	1.98 ± 1.64	−2.5*	+0.5 n.s.
EDC	43.9 ± 10.2	229.4 ± 151.9	2.17 ± 1.84	−2.5*	+0.3 n.s.

Mean ± SD.
* Indicates significant change over time ($p < 0.05$).

In addition to the analysis of the peak-to-peak SRC, we investigated the changes of the area under the MEP curve. Whenever changes of the MEP peak-to-peak amplitudes occur they reflect increases or decreases of corticospinal excitability. Further analysis of the areas under the curve might then disentangle potential neurophysiological mechanisms. Whenever the peak-to-peak changes are paralleled by changes of the areas under the curve as well, these are most likely mediated by the functional recruitment or loss of neurons; whenever the peak-to-peak changes are *not* paralleled by changes of the areas under the curve, these are most likely mediated via increased or decreased synchronization of firing of the stimulated neuronal population (Rösler et al., 2008; Z'Graggen et al., 2005).

The findings in the present study indicated that the BRI intervention was achieving the modulations of corticospinal excitability, i.e. changes in the peak-to-peak curve, by interfering with the synchronicity of the stimulated neuronal pools. More specifically, the BRI intervention seemed to increase the synchronous firing of the neurons mediating the steep part of the SCR, while decreasing the synchronous firing of the neurons mediating the plateau of the SCR, i.e. of the somatosensory and motor cortex, respectively, due to an interaction between the recruitment curve and the map profile (for details see below).

The observed plastic changes in the present study were however robust, i.e. they outlasted the intervention and survived a depotentiation task (Goldsworthy et al., 2015). Previous studies providing visual feedback contingent to brain self-regulation were ambiguous in this regard. While Ros et al. (2010) demonstrated that the increase of corticospinal excitability was also present during rest following the intervention, Pichiorri et al. (2011) and Mokienko et al. (2013) showed the respective changes only during the motor imagery task. This might be related to the fact that these studies applied only visual feedback, whereas particularly somatosensory feedback has been shown to facilitate plasticity (Lewis and Byblow, 2004; Macé et al., 2008; Ridding and Rothwell, 1999). More specifically, the combination of motor imagery and proprioceptive input, but not each of the interventions alone, has been shown to induce a lasting increase of corticospinal excitability (Mrachacz-Kersting et al., 2012; Xu et al., 2014), thus inspiring the combined intervention in the present study as well.

We extend these observations by the novel finding of opposite effects of the BRI intervention for higher stimulation intensities, i.e. a decrease of corticospinal excitability at the SRC plateau, reflecting most likely a rather asynchronous recruitment of neuronal populations and resulting in increased phase cancelation, i.e. chronodispersion of the corticospinal volleys (Magistris et al., 1998; Rösler et al., 2002). Such a dissociation of effects induced by the same intervention might be puzzling at first sight. However, the opposite effects of lower (i.e. steep part of the SRC) and higher (i.e. plateau of the SRC) stimulation intensities might at least in part be explained by opposing excitability changes of the primary motor and the somatosensory cortex influencing the course of the SRC captured with the biphasic pulse waveform applied in this study, revealing an interaction between the recruitment curve and the map profile.

As the stimulation spot for the SRC was located in the central sulcus (see Fig. 5), different cortical areas surrounding this spot are activated depending on the pulse waveform and the stimulation intensity applied. Previous studies have shown that biphasic pulses, as applied in this study, may show some intensity-dependent physiological variability (Maccabee et al., 1998; Orth and Rothwell, 2004; Sommer et al., 2006). While at low stimulus intensities the effects of the anterior–posterior current flow, i.e. pointing towards the somatosensory cortex, were about 20% stronger than the opposing current flow (Maccabee et al., 1998), the specificity with regard to the orientation was less marked at higher intensities (Sommer et al., 2006).

Accordingly, we demonstrated in the present study, that the MEP increases at lower intensities were mapped to the primary somatosensory cortex, which presented with increased corticospinal excitability after the intervention. When increasing the stimulation intensity more brain regions with opposing excitability, i.e. the primary motor cortex, were recruited, thereby limiting or even decreasing the net output. Most other brain-interface based neurofeedback studies used a monophasic TMS pulse form for mapping the effects of the intervention (Pichiorri et al., 2011; Ros et al., 2010; Shindo et al., 2011; Xu et al., 2014) and could possibly miss the finding observed in this study due to the lower neuronal recruitment of monophasic stimulation.

This leads to the question as to why these opposing effects occurred in the primary motor and somatosensory cortex following the intervention, with decreases and increases of corticospinal excitability, respectively. As known from both animal experiments (He et al., 1993, 1995; Huntley and Jones, 1991; Jones and Wise, 1977) and human studies (Kombos et al., 1999; Schmidt et al., 2013; Teitti et al., 2008), corticospinal connections are not limited to the primary motor cortex but extend to different regions of the sensorimotor system. More specifically, about half of the primate brain's pyramidal tract neurons are located in postcentral areas, e.g. the primary somatosensory cortex, sharing functional properties regarding movement-related activity and discharge patterns as a function of muscle strength with precentral pyramidal tract neurons (Russel and DeMyer, 1961; Murray and Coulter, 1981; Fromm and Evarts, 1982). Furthermore, intraoperative electrical stimulation in humans with both mono- and bipolar focal stimulation of the premotor and somatosensory cortex elicited MEPs as well (Kombos et al., 1999). However, due to the rather non-focal nature of TMS a complementary explanation of these findings might be possible. Even if the center of the TMS coil is over the primary somatosensory cortex, and producing larger MEPs than pre-intervention, this doesn't necessarily mean that somatosensory cortex stimulation is producing the descending volley. It could mean that neurons located rather posterior in the motor cortex, but still anterior to the somatosensory cortex, are now more responsive to the magnetic stimulation delivered at the same intensity and location as pre-intervention.

This indicates that combining motor imagery-related β-band ERD with proprioceptive feedback might be sufficient to enhance or even re-distribute corticospinal connectivity, i.e. increasing the effective connectivity of the corticospinal pools located in the motor cortex and/or premotor and somatosensory cortex, respectively. We might speculate that a potential re-distribution is related to the fact that although imagery-related β-band ERD is disinhibiting both motor and somatosensory cortex (Kilavik et al., 2013; Kristeva et al., 2007; Mima et al., 2000; van Wijk et al., 2012), only the latter area is sufficiently modulated by the proprioceptive feedback of the robotic orthosis, i.e. resembling the changes induced by sensory stimulation below motor threshold (Chipchase et al., 2011; Saito et al., 2013; Schabrun et al., 2012; Shitara et al., 2013).

In fact, primary motor cortex excitability crucially depends on the kind of afferent input. If the intensity of peripheral electrical stimulation induces sensory sensation only, motor cortex corticospinal excitability decreases (Chipchase et al., 2011; Schabrun et al., 2012); in contrast, if the peripheral input induces a tonic muscle contraction, then an increase in motor cortex corticospinal excitability occurs (Chipchase et al., 2011; Schabrun et al., 2012). In this vein, if peripheral stimulation is paired with motor imagery, a higher gain in corticospinal excitability can be achieved, but only if the afferent input is above the motor threshold, whereas afferent input that only induces a sensory sensation induces a less pronounced effect (Saito et al., 2013). Moreover, somatosensory stimulation has been shown to activate the caudal part of the motor cortex; whereas afferent stimulation, which induced a visible muscle twitch, activated the rostral part of the motor cortex (Shitara et al., 2013). The posterior shift in the center of gravity in our study – determined by MEP increases mapped to primary somatosensory cortex – is in accordance with these previous findings and suggests that passively opening the hand with a robotic orthosis induces changes similar to sensory stimulation below the motor threshold.

The correlation analysis of ERD and SRC provided converging evidence for this differential modulation of the motor and the somatosensory cortex. Only the latter showed a correlation between the increase of beta-ERD and the MEP increase at lower stimulation intensities suggesting topographic specificity of the BRI intervention.

The study is limited with regard to pinpointing whether these modulations of corticospinal synchronicity took predominantly place on the cortical and/or spinal level; this cannot be answered here, as the spinal excitability has not been investigated in this study. On the one hand, the combination of kinesthetic motor imagery and feedback with passive hand opening induces known muscle activations during the intervention (Solodkin et al., 2004) favoring the spinal level as the substrate for the observed plastic changes. On the other hand, the detected shift in the center of gravity (see below) suggests a cortical involvement as well. Future studies need to address this question by including a specific evaluation of the spinal excitability and researching the different contributions of motor imagery and afferent input separately. It might be advisable for future experiments to acquire cortical maps immediately after the intervention and for longer follow-up periods to probe possible gating effects of BRI training and the time course afterwards, respectively. This will allow probing whether the demonstrated robustness, i.e. surviving a depotentiation task, would translate into long-term stability as well. Moreover, it should be considered in future to randomize the stimulus-response curve and the cortical mapping to avoid potential order effects as well as to include an automated jitter between stimulation pulses to prevent any unintended effects of the TMS measurement.

In conclusion, the presented intervention induced distributed and topographically specific changes of corticospinal connectivity that outlasted the intervention period and have to be considered when used for BRI based neurorehabilitation. This study revealed for the first time (i) muscle specificity of the intervention effects, opposing effects of this intervention within both (ii) the SRC and (iii) the sensorimotor cortex, which were mediated via (iv) increased synchronization of firing of the stimulated neuronal population and not by the recruitment of additional neurons, and moreover (v) a direct correlation between BRI induced ERD changes of individual participants and increased corticospinal excitability.

A possible application of this technique would be a muscle specific priming of subsequent motor learning during physiotherapy as done in previous approaches by combining two independent interventions, i.e. performing brain-interface mediated neurofeedback *before* the following physiotherapy (Ramos-Murguialday et al., 2013; Pichiorri et al., 2015; Naros and Gharabaghi, 2015). These patients, however, might need residual muscle activity to sufficiently participate in the second part, i.e. physiotherapy, of this intervention or would require high levels of support by the therapist.

An alternative application of this technique would offer a framework for restorative therapy by gating simultaneously applied brain stimulation (Gharabaghi et al., 2014). Thereby, this integrated BRI training would become the therapy in itself, i.e. offering assisted movements combined with activity-dependent stimulation paradigms based on intrinsic brain activity. This novel intervention of brain state-dependent cortical stimulation combined with afferent robotic input would be

particularly suited for the many severely affected stroke patients lacking residual hand function.

Acknowledgment

DK, RB and MTL were supported by the Graduate Training Centre of Neuroscience, International Max Planck Research School for Cognitive and Systems Neuroscience, Tuebingen, Germany. AG was supported by grants from the German Research Council [DFG EC 307], and from the Federal Ministry for Education and Research [BFNT 01GQ0761, BMBF 16SV3783, BMBF 0316064B, BMBF 16SV5824].

References

Abbruzzese, G., Assini, A., Buccolieri, A., Marchese, R., Trompetto, C., 1999. Changes of intracortical inhibition during motor imagery in human subjects. Neurosci. Lett. 263 (2–3), 113–116.

Altman, D.G., Bland, J.M., 2011. How to obtain the P value from a confidence interval. BMJ (Clin. Res. Ed.) 343, d2304.

Ang, K.K., Guan, C., Chua, K.S.G., Ang, B.T., Kuah, C.W.K., Wang, C., Phua, K.S., Chin, Z.Y., Zhang, H., 2011. A large clinical study on the ability of stroke patients to use an EEG-based motor imagery brain–computer interface. Clin. EEG Neurosci. 42 (4), 253–258.

Ang, K.K., Chua, K.S., Phua, K.S., Wang, C., Chin, Z.Y., Kuah, C.W., Low, W., Guan, C., 2015 Oct. A Randomized Controlled Trial of EEG-Based Motor Imagery Brain-Computer Interface Robotic Rehabilitation for Stroke. Clin EEG Neurosci 46 (4), 310–320. http://dx.doi.org/10.1177/1550059414522229.

Bauer, R., Gharabaghi, A., 2015a. Estimating cognitive load during self-regulation of brain activity and neurofeedback with therapeutic brain–computer interfaces. Front. Behav. Neurosci. 9, 21. http://dx.doi.org/10.3389/fnbeh.2015.00021.

Bauer, R., Gharabaghi, A., 2015b. Reinforcement learning for adaptive threshold control of restorative brain–computer interfaces: a Bayesian simulation. Front. Neurosci. 9, 36. http://dx.doi.org/10.3389/fnins.2015.00036.

Bauer, R., Fels, M., Vukelić, M., Ziemann, U., Gharabaghi, A., 2015. Bridging the gap between motor imagery and motor execution with a brain-robot interface. Neuroimage. 108, 319–327. http://dx.doi.org/10.1016/j.neuroimage.2014.12.026.

Buch, E., Weber, C., Cohen, L.G., Braun, C., Dimyan, M.A., Ard, T., Mellinger, J., et al., 2008. Think to move: a neuromagnetic brain–computer interface (BCI) system for chronic stroke. Stroke 39 (3), 910–917.

Buch, E.R., Shanechi, A.M., Fourkas, A.D., Weber, C., Birbaumer, N., Cohen, L.G., 2012. Parietofrontal integrity determines neural modulation associated with grasping imagery after stroke. Brain 135 (Pt 2), 596–614.

Chipchase, L.S., Schabrun, S.M., Hodges, P.W., 2011. Corticospinal excitability is dependent on the parameters of peripheral electric stimulation: a preliminary study. Arch. Phys. Med. Rehabil. 92 (9), 1423–1430.

Clarke, Philippa, Black, Sandra E., 2005. Quality of life following stroke: negotiating disability, identity, and resources. J. Appl. Gerontol. 24 (4), 319–336.

Danner, N., Julkunen, P., Könönen, M., Säisänen, L., Nurkkala, J., Karhu, J., 2008. Navigated transcranial magnetic stimulation and computed electric field strength reduce stimulator-dependent differences in the motor threshold. J. Neurosci. Methods 174 (1), 116–122.

Danner, N., Könönen, M., Säisänen, L., Laitinen, R., Mervaala, E., Julkunen, P., 2012. Effect of individual anatomy on resting motor threshold-computed electric field as a measure of cortical excitability. J. Neurosci. Methods 203 (2), 298–304.

Devanne, H., Lavoie, B.A., Capaday, C., 1997. Input–output properties and gain changes in the human corticospinal pathway. Exp. Brain Res. 114 (2), 329–338.

Di Lazzaro, V., Oliviero, A., Mazzone, P., Insola, A., Pilato, F., Saturno, E., Accurso, A., Tonali, P., Rothwell, J.C., 2001. Comparison of descending volleys evoked by monophasic and biphasic magnetic stimulation of the motor cortex in conscious humans. Exp. Brain Res. 141 (1), 121–127 (Nov.).

Dobkin, B.H., 2005. Clinical practice. Rehabilitation after stroke. N. Engl. J. Med. 352 (16), 1677–1684 (Apr 21).

Fromm, C., Evarts, E.V., 1982. Pyramidal tract neurons in somatosensory cortex: central and peripheral inputs during voluntary movement. Brain Res. 238 (1), 186–191 (Apr 22).

Gharabaghi, A., Kraus, D., Leão, M.T., Spüler, M., Walter, A., Bogdan, M., Rosenstiel, W., Naros, G., Ziemann, U., 2014. Coupling brain–machine interfaces with cortical stimulation for brain-state dependent stimulation: enhancing motor cortex excitability for neurorehabilitation. Front. Hum. Neurosci. 8, 122 (Mar 5).

Goldsworthy, M.R., Müller-Dahlhaus, F., Ridding, M.C., Ziemann, U., 2015. Resistant against de-depression: LTD-like plasticity in the human motor cortex induced by spaced cTBS. Cereb. Cortex 25 (7), 1724–1734. http://dx.doi.org/10.1093/cercor/bht353 (Jul).

Gomez-Rodriguez, M., Peters, J., Hill, J., Schölkopf, B., Gharabaghi, A., Grosse-Wentrup, M., 2011. Closing the sensorimotor loop: haptic feedback facilitates decoding of motor imagery. J. Neural Eng. 8 (3), 036005.

Groppa, S., Oliviero, A., Eisen, A., Quartarone, A., Cohen, L.G., Mall, V., Kaelin-Lang, A., et al., 2012. A practical guide to diagnostic transcranial magnetic stimulation: report of an IFCN committee. Clin. Neurophysiol. 123 (5), 858–882.

He, S.Q., Dum, R.P., Strick, P.L., 1993. Topographic organization of corticospinal projections from the frontal lobe: motor areas on the lateral surface of the hemisphere. J. Neurosci. 13 (3), 952–980.

He, S.Q., Dum, R.P., Strick, P.L., 1995. Topographic organization of corticospinal projections from the frontal lobe: motor areas on the medial surface of the hemisphere. J. Neurosci. 15 (5 Pt 1), 3284–3306.

Houdayer, E., Degardin, A., Cassim, F., Bocquillon, P., Derambure, P., Devanne, H., 2008. The effects of low- and high-frequency repetitive TMS on the input/output properties of the human corticospinal pathway. Exp. Brain Res. 187 (2), 207–217.

Huber, P.J., 1981. Robust Statistics. John Wiley & Sons, Inc., Hoboken, NJ.

Huntley, G.W., Jones, E.G., 1991 Aug. Relationship of intrinsic connections to forelimb movement representations in monkey motor cortex: a correlative anatomic and physiological study. J Neurophysiol 66 (2), 390–413.

Jensen, O., Mazaheri, A., 2010. Shaping functional architecture by oscillatory alpha activity: gating by inhibition. Front. Hum. Neurosci. 4, 186.

Jones, E.G., Wise, S.P., 1977 Oct 15. Size, laminar and columnar distribution of efferent cells in the sensory-motor cortex of monkeys. J. Comp. Neurol 175 (4), 391–438.

Kaelin-Lang, A., Luft, A.R., Sawaki, L., Burstein, A.H., Sohn, Y.H., Cohen, L.G., 2002. Modulation of human corticomotor excitability by somatosensory input. J. Physiol. 540 (Pt 2), 623–633.

Kilavik, B.E., Zaepffel, M., Brovelli, A., MacKay, W.A., Riehle, A., 2013. The ups and downs of β oscillations in sensorimotor cortex. Exp. Neurol. 245, 15–26.

Kombos, T., Suess, O., Kern, B.C., Funk, T., Hoell, T., Kopetsch, O., Brock, M., 1999. Comparison between monopolar and bipolar electrical stimulation of the motor cortex. Acta Neurochir. (Wien) 141 (12), 1295–1301.

Kraus, D., Gharabaghi, A., 2015. Projecting navigated TMS sites on the gyral anatomy decreases inter-subject variability of cortical motor maps. Brain Stimul. 8 (4), 831–837. http://dx.doi.org/10.1016/j.brs.2015.03.006 (Jul–Aug).

Kristeva, R., Patino, L., Omlor, W., 2007. Beta-range cortical motor spectral power and corticomuscular coherence as a mechanism for effective corticospinal interaction during steady-state motor output. Neuroimage 36, 785–792.

Kutner, N.G., Zhang, R., Butler, A.J., Wolf, S.L., Alberts, J.L., 2010. Quality-of-life change associated with robotic-assisted therapy to improve hand motor function in patients with subacute stroke: a randomized clinical trial. Phys. Ther. 90 (4), 493–504 (Apr).

Langhorne, P., Coupar, F., Pollock, A., 2009. Motor recovery after stroke: a systematic review. Lancet Neurol. 8 (8), 741–754.

Lewis, G.N., Byblow, W.D., 2004. The effects of repetitive proprioceptive stimulation on corticomotor representation in intact and hemiplegic individuals. Clin. Neurophysiol. 115 (4), 765–773.

Maccabee, P.J., Nagarajan, S.S., Amassian, V.E., Durand, D.M., Szabo, A.Z., Ahad, A.B., Cracco, R.Q., Lai, K.S., Eberle, L.P., 1998. Influence of pulse sequence, polarity and amplitude on magnetic stimulation of human and porcine peripheral nerve. J. Physiol. 513 (Pt 2), 571–585 (December).

Macé, M.J.M., Levin, O., Alaerts, K., Rothwell, J.C., Swinnen, S.P., 2008. Corticospinal facilitation following prolonged proprioceptive stimulation by means of passive wrist movement. J. Clin. Neurophysiol. 25 (4), 202–209.

Magistris, M.R., Rösler, K.M., Truffert, A., Myers, J.P., 1998. Transcranial stimulation excites virtually all motor neurons supplying the target muscle. A demonstration and a method improving the study of motor evoked potentials. Brain 121 (Pt 3), 437–450 (March).

McFarland, D.J., Wolpaw, J.R., 2008. Sensorimotor rhythm-based brain–computer interface (BCI): model order selection for autoregressive spectral analysis. J. Neural Eng. 5 (2), 155–162.

McFarland, D.J., Miner, L.A., Vaughan, T.M., Wolpaw, J.R., 2000. Mu and beta rhythm topographies during motor imagery and actual movements. Brain Topogr. 12 (3), 177–186.

Mehrholz, J., Hadrich, A., Platz, T., Kugler, J., Pohl, M., 2012. Electromechanical and robot-assisted arm training for improving generic activities of daily living, arm function, and arm muscle strength after stroke. Cochrane Database Syst. Rev. 6, CD006876.

Mima, T., Steger, J., Schulman, A.E., Gerloff, C., Hallett, M., 2000. Electroencephalographic measurement of motor cortex control of muscle activity in humans. Clin. Neurophysiol. 111, 326–337.

Mokienko, O.A., Chervyakov, A.V., Kulikova, S.N., Bobrov, P.D., Chernikova, L.A., Frolov, A.A., Piradov, M.A., 2013. Increased motor cortex excitability during motor imagery in brain–computer interface trained subjects. Front. Comput. Neurosci. 7, 168.

Möller, C., Arai, N., Lücke, J., Ziemann, U., 2009. Hysteresis effects on the input–output curve of motor evoked potentials. Clin. Neurophysiol. 120 (5), 1003–1008.

Mrachacz-Kersting, N., Kristensen, S.R., Khan Niazi, I., Farina, D., 2012. Precise temporal association between cortical potentials evoked by motor imagination and afference induces cortical plasticity. J. Physiol. 590 (Pt 7), 1669–1682.

Murray, E.A., Coulter, J.D., 1981. Organization of corticospinal neurons in the monkey. J. Comp. Neurol. 195 (2), 339–365 (Jan 10).

Naros, G., Gharabaghi, A., 2015. Reinforcement learning of self-regulated β-oscillations for motor restoration in chronic stroke. Front. Hum. Neurosci. 9, 391. http://dx.doi.org/10.3389/fnhum.2015.00391.

Oldfield, R.C., 1971. The assessment and analysis of handedness: the Edinburgh inventory. Neuropsychologia 9 (1), 97–113.

Orth, M., Rothwell, J.C., 2004. The cortical silent period: intrinsic variability and relation to the waveform of the transcranial magnetic stimulation pulse. Clin. Neurophysiol. 115 (5), 1076–1082.

Pichiorri, F., De Vico, Fallani F., Cincotti, F., Babiloni, F., Molinari, M., Kleih, S.C., Neuper, C., Kübler, A., Mattia, D., 2011. Sensorimotor rhythm-based brain–computer interface training: the impact on motor cortical responsiveness. J. Neural Eng. 8 (2), 025020.

Pichiorri, F., Morone, G., Petti, M., Toppi, J., Pisotta, I., Molinari, M., Paolucci, S., Inghilleri, M., Astolfi, L., Cincotti, F., et al., 2015. Brain–computer interface boosts motor imagery practice during stroke recovery. Ann. Neurol. 77, 851–865.

Prasad, G., Herman, P., Coyle, D., McDonough, S., Crosbie, J., 2010. Applying a brain–computer interface to support motor imagery practice in people with stroke for upper limb recovery: a feasibility study. J. Neuroeng. Rehabil. 7, 60.

Raffin, E., Pellegrino, G., Di Lazzaro, V., Thielscher, A., Siebner, H.R., 2015. Bringing transcranial mapping into shape: sulcus-aligned mapping captures motor somatotopy in human primary motor hand area. Neuroimage. 120, 164–175 (Jul 15).
Ramos-Murguialday, A., Brötz, D., Rea, M., Läer, L., Yilmaz, Ö., Brasil, F.L., Liberati, G., et al., 2013. Brain–machine interface in chronic stroke rehabilitation: a controlled study: BMI in chronic stroke. Ann. Neurol. 74 (1), 100–108.
Ridding, M.C., Rothwell, J.C., 1999. Afferent input and cortical organisation: a study with magnetic stimulation. Exp. Brain Res. 126 (4), 536–544.
Roosink, M., Zijdewind, I., 2010. Corticospinal excitability during observation and imagery of simple and complex hand tasks: implications for motor rehabilitation. Behav. Brain Res. 213 (1), 35–41.
Ros, T., Munneke, M.A.M., Ruge, D., Gruzelier, J.H., Rothwell, J.C., 2010. Endogenous control of waking brain rhythms induces neuroplasticity in humans. Eur. J. Neurosci. 31 (4), 770–778.
Rosenkranz, K., Pesenti, A., Paulus, W., Tergau, F., 2003. Focal reduction of intracortical inhibition in the motor cortex by selective proprioceptive stimulation. Exp. Brain Res. 149 (1), 9–16.
Rosenkranz, K., Rothwell, J.C., 2003 Sep 1. Differential effect of muscle vibration on intracortical inhibitory circuits in humans. J Physiol 551 (Pt 2), 649–660.
Rosenkranz, K., Rothwell, J.C., 2012 Jun 27. Modulation of proprioceptive integration in the motor cortex shapes human motor learning. J Neurosci 32 (26), 9000–9006. http://dx.doi.org/10.1523/JNEUROSCI.0120-12.2012.
Rösler, K.M., Petrow, E., Mathis, J., Arányi, Z., Hess, C.W., Magistris, M.R., 2002. Effect of discharge desynchronization on the size of motor evoked potentials: an analysis. Clin. Neurophysiol. 113 (11), 1680–1687.
Rösler, K.M., Roth, D.M., Magistris, M.R., 2008. Trial-to-trial size variability of motor-evoked potentials. a study using the triple stimulation technique. Exp. Brain Res. 187 (1), 51–59.
Rossi, S., Hallett, M., Rossini, P.M., Pascual-Leone, A., Safety of TMS Consensus Group, 2009. Safety, ethical considerations, and application guidelines for the use of transcranial magnetic stimulation in clinical practice and research. Clin. Neurophysiol. 120 (12), 2008–2039.
Rossini, P.M., Rossi, S., Pasqualetti, P., Tecchio, F., 1999. Corticospinal excitability modulation to hand muscles during movement imagery. Cereb. Cortex 9 (2), 161–167.
Russel, J.R., Demyer, W., 1961. The quantitative corticoid origin of pyramidal axons of *Macaca* rhesus. With some remarks on the slow rate of axolysis. Neurology 11, 96–108 (Feb).
Saito, K., Yamaguchi, T., Yoshida, N., Tanabe, S., Kondo, K., Sugawara, K., 2013. Combined effect of motor imagery and peripheral nerve electrical stimulation on the motor cortex. Exp. Brain Res. 227 (3), 333–342.
Schabrun, S.M., Ridding, M.C., Galea, M.P., Hodges, P.W., Chipchase, L.S., 2012. Primary sensory and motor cortex excitability are co-modulated in response to peripheral electrical nerve stimulation. PLoS One 7 (12), e51298.
Schalk, G., McFarland, D.J., Hinterberger, T., Birbaumer, N., Wolpaw, J.R., 2004. BCI2000: a general-purpose brain–computer interface (BCI) system. IEEE Trans. Biomed. Eng. 51 (6), 1034–1043.
Schmidt, S., Fleischmann, R., Bathe-Peters, R., Irlbacher, K., Brandt, S.A., 2013. Evolution of premotor cortical excitability after cathodal inhibition of the primary motor cortex: a sham-controlled serial navigated TMS study. PLoS One 8 (2), e57425.
Shindo, K., Kawashima, K., Ushiba, J., Ota, N., Ito, M., Ota, T., Kimura, A., Liu, M., 2011. Effects of neurofeedback training with an electroencephalogram-based brain–computer interface for hand paralysis in patients with chronic stroke: a preliminary case series study. J. Rehabil. Med. 43 (10), 951–957.
Shitara, H., Shinozaki, T., Takagishi, K., Honda, M., Hanakawa, T., 2013. Movement and afferent representations in human motor areas: a simultaneous neuroimaging and transcranial magnetic/peripheral nerve-stimulation study. Front. Hum. Neurosci. 7, 554.
Solodkin, A., Hlustik, P., Chen, E.E., Small, S.L., 2004. Fine modulation in network activation during motor execution and motor imagery. Cereb. Cortex 14 (11), 1246–1255.
Sommer, M., Alfaro, A., Rummel, M., Speck, S., Lang, N., Tings, T., Paulus, W., 2006. Half sine, monophasic and biphasic transcranial magnetic stimulation of the human motor cortex. Clin. Neurophysiol. 117 (4), 838–844.
Stinear, C.M., Byblow, W.D., 2004. Modulation of corticospinal excitability and intracortical inhibition during motor imagery is task-dependent. Exp. Brain Res. 157 (3), 351–358.
Stinear, C.M., Byblow, W.D., Steyvers, M., Levin, O., Swinnen, S.P., 2006. Kinesthetic, but not visual, motor imagery modulates corticomotor excitability. Exp. Brain Res. 168 (1–2), 157–164.
Teitti, S., Määttä, S., Säisänen, L., Könönen, M., Vanninen, R., Hannula, H., Mervaala, E., Karhu, J., 2008. Non-primary motor areas in the human frontal lobe are connected directly to hand muscles. NeuroImage 40 (3), 1243–1250.
Todd, G., Rogasch, N.C., Flavel, S.C., Ridding, M.C., 2009. Voluntary movement and repetitive transcranial magnetic stimulation over human motor cortex. J. Appl. Physiol. 106 (5), 1593–1603.
Touge, T., Gerschlager, W., Brown, P., Rothwell, J.C., 2001. Are the after-effects of low-frequency rTMS on motor cortex excitability due to changes in the efficacy of cortical synapses? Clin. Neurophysiol. 112 (11), 2138–2145.
van Wijk, B.C., Beek, P.J., Daffertshofer, A., 2012. Neural synchrony within the motor system: what have we learned so far? Front. Hum. Neurosci. 6.
Vukelić, M., Gharabaghi, A., 2015a. Oscillatory entrainment of the motor cortical network during motor imagery is modulated by the feedback modality. Neuroimage 111C, 1–11 (Feb 7).
Vukelic, M., Gharabaghi, A., 2015b. Self-regulation of circumscribed brain activity modulates spatially selective and frequency specific connectivity of distributed resting state networks. Front. Behav. Neurosci. 9, 181. http://dx.doi.org/10.3389/fnbeh.2015.00181.
Vukelić, M., Bauer, R., Naros, G., Naros, I., Braun, C., Gharabaghi, A., 2014. Lateralized alpha-band cortical networks regulate volitional modulation of beta-band sensorimotor oscillations. NeuroImage 87, 147–153.
Wassermann, E.M., McShane, L.M., Hallett, M., Cohen, L.G., 1992. Noninvasive mapping of muscle representations in human motor cortex. Electroencephalogr. Clin. Neurophysiol. 85 (1), 1–8.
Xu, R., Jiang, N., Mrachacz-Kersting, N., Lin, C., Asin Prieto, G., Moreno, J.C., Pons, J.L., Dremstrup, K., Farina, D., 2014. A closed-loop brain–computer interface triggering an active ankle–foot orthosis for inducing cortical neural plasticity. IEEE Trans. Biomed. Eng. 61 (7), 2092–2101.
Z'Graggen, W.J., Humm, A.M., Durisch, N., Magistris, M.R., Rösler, K.M., 2005. Repetitive spinal motor neuron discharges following single transcranial magnetic stimuli: a quantitative study. Clin. Neurophysiol. 116 (7), 1628–1637.
Ziemann, U., Siebner, H.R., 2008. Modifying motor learning through gating and homeostatic metaplasticity. Brain Stimul. 1 (1), 60–66.
Ziemann, U., Lönnecker, S., Steinhoff, B.J., Paulus, W., 1996. Effects of antiepileptic drugs on motor cortex excitability in humans: a transcranial magnetic stimulation study. Ann. Neurol. 40 (3), 367–378.